THE RECIPROCAL PRODUCTIVITY INDEX METHOD, A GRAPHICAL WELL PERFORMANCE SIMULATOR

by
James W. Crafton
Snyder Oil Corporation

Abstract

The ability to estimate descriptive engineering parameters, such as permeability, and to generate production forecasts and reserves based on those parameters, without the cost of full numerical simulation or extended buildup tests, is provided by the Reciprocal Productivity Index graphical production analysis method. The method's theoretical basis arises from the fact that traditional constant rate or constant pressure (potential) boundary conditions are sufficient, but that the necessary boundary condition only requires that the sandface transmissibility remain constant over time. With that difference, it is possible to accurately evaluate production histories, in which both the rate and pressure are varying over time, using traditional well testing methods. Examples for both oil and gas wells demonstrate the interpretive capability and limitations.

Introduction

The engineering evaluation of production history data from oil and gas wells can be very beneficial. Economics always mitigate against extended build-up tests, whose results are often optimistic estimators of well performance. The need to produce a well as soon as stimulation is finished makes a performance evaluation tool capable of offering early interpretation valuable. It is also very helpful to have that performance evaluation tool coupled with a production forecasting and reserves estimation capability using traditional reservoir engineering parameters. Those capabilities provide a natural process for problem diagnosis. As the user becomes comfortable with these methods, many other applications become apparent.

Many methods have been developed to address those lofty objectives, such as automatic history matching with numerical simulation, the reciprocal of production rate versus square root or log of time, or the type curve analysis of production decline curves. The Reciprocal Productivity Index method joins that group. There are two major differences with the methods to be discussed here and the other methods: 1) the Reciprocal Productivity Index method recognizes the interpretability of data in which either or both rate and pressure are changing without the need for convolution or full numerical simulation, and 2) the history matching process is graphical, although it can be preconditioned by automatic methods.

Finally, a persistent issue exists as to the interpretability of production data, when compared to build-up test data. This paper will briefly show that exactly the same fundamental theory governs both. Clearly,

when only one of the independent variables (rate or pressure) is analyzed, assuming the other constant, the analysis of production data becomes more subjective. Whereas, a build-up test, by its very nature, incorporates both variables. One of the examples will demonstrate the consistency of the RPI and build-up analyses when a complete data set is available.

Prior Literature

The very earliest work in this area was provided by Gladfelter, *etal.*[1], which explored the accuracy of interpretation for high permeability reservoirs. Work by Neal and Mian[2] was initiated to find an evaluation procedure for low permeability reservoirs such as the "J Sand" in Colorado's DJ Basin. Their method showed the usability of reciprocal rate versus square root of time for these low permeability systems. Reitman[3] showed that log of time and reciprocal rate was meaningful. His analysis suggests that the use of superposition or convolution is necessary to treat data in which the pressure changes with time. The evaluation of log of rate versus time production decline curves was first made practical by Fetkovich[4].

The use of numerical simulation and history matching procedures has a long history. A recent automatic history matching procedure[5] and older ones[6,7] performing much the same function, show the ability to solve the evaluation/forecasting problem. However, Garcia[8] has shown the sensitivity and nature of the problems which arise with automatic history matching procedures used with noisy data.

A Reason for the RPI (An Editorial Comment)

The experience of the author with various well performance analysis tools led to the search for a tool to evaluate both oil and gas wells. It is necessary to evaluate data sets which invariably contain very large amounts of noise, and may or may not include pressure histories. The tool must be able to estimate engineering parameters such as permeability, drained area, etc. which can be used to provide the basis for both performance assessment and production forecasting. The difficulty with automatic history matching with very noisy data is the consistent determination of a reasonably unique solution. Whereas the ability of a competent engineer to perform intuitive pattern recognition is well recognized.

Theoretical Basis for RPI

In Appendix A, an abbreviated derivation of the fundamental theory for the Reciprocal Productivity Index method is provided. The derivation shown is for a linear flow regime, but an analogous derivation can be obtained for any geometry or even for finite difference or variational numerical simulations[9]. In essence, the difference between the theory employed by the Reciprocal Productivity Index method and that of other treatments is the generalization of the so-called "interior boundary condition". Virtually all authors impose a boundary constraint of either constant mass rate or constant pressure over time. Then the derivation for a solution proceeds using that formulation to evaluate the second constant of integration (if formal integration is employed)[1,3,10,11,12,13,14].

If the integration is conducted in terms of dimensionless parameters, i.e. dimensionless time, pressure and distance, the boundary conditions must also be cast into that setting. One discovers that pre-disposing the "interior boundary condition" with an assumption of constant rate or pressure is, in fact, unnecessary. In dimensionless form, regardless of the prior choice, the "interior boundary condition" is a constant only dependent on the geometry of that boundary and region of integration. Therefore, while the assumption of either constant rate or pressure is sufficient, it is not necessary, in a mathematical sense. The necessary "interior boundary condition" simply requires that the derivative of dimensionless pressure with dimensionless distance be constant over time.

In other words, that "interior boundary condition" can be interpreted to say that rate and/or pressure can vary with time at the wellbore in such manner that the space derivative of the reciprocal of the productivity index $\{(P_i - P_w(t))$ over $q(t)\}$ be constant. A corollary to that is the requirement that both the permeability-thickness product and density at standard conditions remain constant over time.

That result has several very important consequences! The most immediate result is that rate and pressure data which vary simultaneously can be treated without superposition or convolution in a meaningful way. (In fact, with very noisy production data, superposition or convolution clearly becomes a source of error, because that noise gives a signature of apparently higher permeability in the system[8].) Violation of the derivative being constant in space gives rise to a term exactly analogous to the vanEverdingen skin[5]. Variation of the sandface permeability-thickness product, fracture length or produced fluid composition over time have characteristic signatures, because they violate the constancy requirement.

Because of the obvious similarity to classic pressure transient theory, many, if not all, the same techniques are applicable. Rather than employ a Horner[11] analysis, the appropriate method for the determination of the permeability-thickness product is the Miller-Dyes-Hutchinson[12] plot, using the reciprocal of the productivity index versus log of time. Skin, the onset of pseudo-steady state and other performance related diagnostics can be observed on that graph. By "merging" the Agarwal[13] and the Gringarten[16] type curves, the transitions from fracture dominated to middle time/reservoir dominated to late time/pseudo-steady state dominated behavior can be observed. The log-log mapping of the data represents a specific solution to the diffusivity equation and its boundary conditions, that is different than the semi-log form. This is a direct way to improve the uniqueness of the parameter estimation, since a valid set of descriptive parameters should satisfy both. The third mapping is the Cartesian (unmapped) graph of the reciprocal of the productivity index versus time. This setting is useful for the further confirmation of uniqueness. It also provides confirmation that late-time behavior is, in fact, due to reservoir boundedness, rather than interference or production operations problems.

Examples

The following examples are constructed with data from real wells which has been altered with the intent to disguise their identity, but preserve the information contained in the data. Further, the examples were selected for their demonstration of specific kinds of situations.

Example #1.

The first example is a gas well which was repeatedly flow tested, each flow period followed by a buildup test. As can be seen from Fig. 1, the production of each flow period was dropping sharply. Figs. 2 and 3 show the Horner plot for two of the three buildups conducted (data for the third is unavailable). Notice that even though the effective permeability appeared to increase slightly, the P^* for the first test is approximately 170 PSI higher than the second. One would be inclined to interpret that response as a severely bounded reservoir, which the operator did. Although the log-log plots for the buildups are not included here, they showed significant wellbore storage.

The RPI analysis method was employed to confirm the original interpretation. The pressure response varied from over 1100 PSIA to 250 PSIA during the flow periods. The rates are shown on Fig. 1, along with the flowing pressures. Fig. 4 is the RPI version of an MDH semi-log plot of reciprocal productivity index versus log of time. Notice that the slopes of the three flow periods are approximately equal, but displaced sequentially upward. That behavior would suggest that each of the flow periods was controlled by about the same reservoir permeability-thickness product, but each period experienced greater damage. From the Agarwal-Gringarten plot (Fig. 5), the log of RPI versus log of time shows that each subsequent flow period exhibits a lower F_{CD}, consistent with the increasing damage interpretation. Notice that there is no evidence of wellbore storage, even though the data points are recorded every two hours. More importantly, notice that none of the log-log slopes show any evidence of turning to the unit slope, characteristic of a bounded flow system. The Cartesian plot (Fig. 6), which is diagnostic of boundedness if the data exhibits a linear character, confirms the interpretation that no boundaries have been encountered.

Review of the well operations history showed that a very small foam fracture stimulation had been performed, with no post-stimulation clean-up prior to the production testing. Further, at the conclusion of both buildups, the well had to be killed to remove the pressure bombs and swabbed back to production. Table 1 provides a comparison of the interpretations of the buildups and the RPI method. The core permeability corrected to *in situ* conditions is not shown, but was consistent with the other results. It should be noted that when this relatively noise-free data set was interpreted with full rate superposition, the effective fracture length appeared to be almost twice as long, or the effective permeability appeared to be about fifty percent greater. (Noise always gives the signature of increased apparent permeability or fracture length)

Example #2.

The second example is a well in which the completion was conducted with three separate fracture stimulation and clean-up flowbacks, then finally commingled. The production and pressure history for the stages of the well are shown on Fig. 7. Notice on the RPI/MDH plot (Fig. 8) that the cleanup of the first stage could be interpreted to have a steeper slope consistent with its smaller gross interval, and clearly has a larger positive skin. The second stage has a shallower slope probably indicative of its larger interval, and apparently better stimulation. The third stage is almost indistinguishable from the commingled performance. When commingled, the three stages have a combined early performance suggestive of contribution only

coming from the last stimulation stage..

The production data after commingling exhibits significant fluctuations. That is consistent with fluid lifting problems. Notice on the log-log plot (Fig. 9) that the later data seems to be turning onto a pseudo-steady-state line, indicative of a bounded reservoir. Fig. 10, the pseudo-steady state graph, appears to support that, until the very end of the data set, when compression was installed. A significant increase in liquids production occurred. The RPI indicates that the well returned to virtually its original unbounded behavior, further confirmation of liquids lifting issues. Also notice the presence of "fine-scale" noise in the production data occurring on about weekly cycles. Its cause is unknown.

Example #3.

This gas well has a very simple single interval completion in a zone suspected of having small reservoir compartments. The production history (lower line) and RPI match (upper line) are shown on Fig. 11. Review of the RPI/MDH plot (Fig. 12) raises an issue of which slope to choose as that which is representative of the reservoir. Concern also arises from the fact that the later slope is associated with a much noisier dataset, frequently an indicator of liquids management problems. If this later slope is chosen, one finds that, when the data is plotted on the log-log plot (Fig. 13), that same interval of data is too steep to match any of the type curve lines, regardless of conductivity or fracture length. When the earlier slope is chosen, a reasonable fracture length and log-log slope match are achieved.

This and companion wells persistently exhibit the behavior of an infinite conductivity fracture. It is known from tracer surveys that the fractures frequently have extensive height growth. Therefore, the conclusion has been drawn that the infinite acting behavior is actually diagnostic of out-of-zone fracturing.

The data later in time suggest the onset to pseudo-steady-state. However, the fact that the pseudo-steady-state plot (Fig. 14) does not exhibit a straight line in late time is inconsistent. There are three possible explanations: 1) the reservoir is indeed bounded, but of a very long rectangular shape requiring the use of Matthews, Brons and Hazebroek shape corrections, 2) a time dependent damage due to liquids accumulation occurred, or 3) the boundary to the system is actually pressure sensitive and expandable. As support for the latter hypothesis, notice the plateaus that are exhibited on Fig. 13 during the late time where the RPI value remains virtually constant for extended periods of time. That signature is relatively common and could be construed to reflect an increasing drained area over time.

Example #4.

The primary purpose for including this example is to demonstrate that sucker rod pumped oil wells even provide interpretable datasets. Although the well produces from several commingled zones, the effective permeability interpreted from the RPI compares favorably with that determined from buildup tests. The RPI does not show the drainage that was observed in one of the zones of one buildup test. However, it does show the onset to failure of the pump at about 32 days on Fig. 15, and return to near-normal production after the repair. The fact that the well returned to its pre-repair performance condition is

supported by Fig. 16 after a log time value of about 1.52. If the well had been significantly impaired, the line would have shifted upward, while maintaining about the same slope. Fig. 17 does not yet exhibit the interference known to exist in the well, probably due to masking by cross-flow.

Conclusions

The theory behind the Reciprocal Productivity Index method provides a robust technique suitable for the rapid interpretation of noisy production data from stimulated oil and gas wells producing multiphase fluid streams. The use of log-log (Agarwal-Gringarten), semi-log (MDH) and Cartesian (PSS) plots simultaneously, permits the interpretation of early, middle and late-time data and provides the ability to significantly improve the uniqueness of the estimated parameters. The method has been demonstrated to give estimates of permeability, fracture length and drained area comparable to those obtained from buildups and core, even when both the rate and pressure are varying significantly throughout the flow period. Better comparisons are achieved when superposition or convolution is not used, particularly with noisy data.

The RPI method provides the basis for production forecasting and reserves estimation based on reservoir engineering parameters, whose reasonableness is easily tested. Those forecasts can also test the benefit of changes in operating pressure or stimulation. When noise-free datasets are available, it is possible to make reasonable estimates of the effective relative permeability to each fluid phase. Every pressure transient theoretician should be enormously offended by the violation of the long-held requirement for constant rate or pressure boundary conditions.

References

1. Matthews, C.S., Russell, D.G., Pressure Buildup and Flow Tests in Wells, Monograph Series, Vol. 1, SPE of AIME, Dallas, TX, (1967).

2. Neal, D.B., Mian, M.A., "Early-Time Tight Gas Production Forecasting Technique Improves Reserves and Reservoir Description", SPE Preprint No. 16432, presented at the SPE Annula Tech. Conf. and Exhib., New Orleans, LA, Oct. 5-8, 1986; SPE Form. Eval. (Mar., 1989) 25-32.

3. Reitman, N.D., "Determining Permeability,Skin Effect and Drainage Area from the Inverted Decline Curve (IDC)", SPE Preprint No. 29464, presented at the Production Operations Symposium, Oklahoma City, OK, April 2-4, 1995.

4. Fetkovich, M.J., "Decline Curve Analysis using Type Curves", J. Pet. Tech. (June, 1980) 1065-1077; Trans. vol. 269.

5. Powell, B., "PROMAT™ for Windows", S.A. Holditch & Assoc., Inc., Houston, TX. (June, 1995).

6. Crafton, J.W., Poundstone, D.J. and Brown, C.A., "A Practical Model for Evaluating a Well Producing from a Tight Gas Formation", SPE/DOE Preprint No. 10841, presented at the SPE/DOE Unconventional Gas Recovery Symposium, Pittsburgh, PA, May 16-18, 1982.

7. Poundstone, D.J., Crafton, J.W., Brown, C.A., "Practical Applications for a Gas Well Model with a Fracture", SPE Preprint No. 11102, presented at the 57th Annual Fall Tech. Conf. and Exhib., New Orleans, LA, Sept. 26-29, 1982.

8. Garcia, F., The Effect of Noisy Historical Data on an Automatic History Matching Procedure, T-3278, Thesis submitted in partial fulfillment of requirements at Colorado School of Mines, Petroleum Engineering Dept. (Nov. 24, 1986).

9. Harris, C.D., Personnal Communication and Theoretical Notes, Univ. of Tulsa, Dept. of Mathematics (1975).

10. Earlougher, R.C., Jr., Advances in Well Test Analysis, Monograph #5, Soc. of Petr. Engrs, Dallas, 1977.

11. Horner, D.R., "Pressure Build-up in Wells", Proc., 3rd World Petr. Cong., E.J. Brill, Leiden (1951) Vol. II, p. 503.

12. Miller, C.C., Dyes, A.B., Hutchinson, C.A., Jr., "The Estimation of Permeability and Reservoir Pressure from Bottom Hole Pressure Buildup Characteriestics", Trans., AIME (1950) 189, 91-104.

13. Agarwal, R.G., Carter, R.D., Pollock, C.B., "Evaluation and Performance Predictino of Low-Permeability Gas Wells Stimulated by Massive Hydraulic Fracturing", J. Petr. Tech. (Mar., 1979) 362-372D: Trans. AIME, Vol. 267.

14. Lee, W.J.: Well Testing, Soc. of Petr. Engrs., Dallas, TX (1982), pg. 13.

15. van Everdingen, A.F., Hurst, W., "The Application of the LaPlace Transformation to Flow Problems in Reservoirs", Trans. AIME (1949) Vol. 185, 305-324.

16. Gringarten, A.C., Ramey, H.J., Jr., Raghavan, R., "Unsteady-State Pressure Distributions Created by a Well with a single Infinite-Conductivity Vertical Fracture", Soc. Petr. Engr. J. (Aug., 1974) 347-360: Trans., AIME, Vol. 257.

17. Wylie, C.R., Jr.: Advanced Engineering Mathematics, McGraw-Hill Book Co., New York (1960) 2, pg. 289.

Appendix A: Derivation for the Reciprocal Productivity Index Method

The Field Equation.

The usual assumptions for the diffusivity equation in a homogeneous porous, permeable material apply, which yields, in this case for a linear geometry:

1) $$\frac{\partial^2 \Psi}{\partial x^2} = -\frac{\Phi \mu\ c}{k} \frac{\partial \Psi}{\partial t}$$

where Ψ represents the definition of pseudo-potential:

2) $$\Psi = \int \frac{\rho}{\mu} dP$$

Realizing that an exactly analogous derivation can be achieved for radial coordinates, the following dimensionless definitions are made for a linear flow regime. The dimensionless distance will be defined

3) $$x_D = \frac{4x}{x_f}$$

as:
Dimensionless time will be defined as:

4) $$t_D = \frac{16\,kt}{\Phi \mu\ c\, x_f^2}$$

Dimensionless potential drop is:

5) $$\Psi_D = \frac{2\pi\ kh\left(\Psi_i - \Psi_w(t)\right)}{q_s(t)\,\rho_s}$$

which if the viscosity and density are constant yields the usual definition of dimensionless pressure drop:

6) $$P_D = \frac{2\pi\ kh\left(P_i - P_w(t)\right)}{q_s(t)\,B_g\ \mu_g}$$

Combining the dimensionless groups in the linear diffusivity equation yields:

7) $$\frac{\partial^2 \Psi_D}{\partial x_D^2} = -\frac{\partial \Psi_D}{\partial t_D}$$

The Boundary Conditions.

Although many authors show three boundary conditions, in the dimensionless space, it is sufficient to define only two. The first states that the initial potential (pressure) can be found somewhere in the semi-infinite reservoir dependent on the elapsed time. In other words, at the initial time the initial potential will

exist at the wellbore, but later it will be found a predictable distance further away. It is stated mathematically as: $\Psi_D \forall 0$ as $t_D \forall 0$. The second boundary condition establishes the states of the "edge" of the semi-infinite region and simply requires that the equation of motion applies at the inner (wellbore or fracture face) boundary, which is:

8) $$v\rho\ A = -\frac{k\rho\ A}{\mu}\frac{dP_w}{dx}$$

which changes with the substitution of the pseudo-potential definition:

9) $$q_s\ \rho_s = -kA\frac{d\Psi_w}{dx}$$

and with the substitution of the dimensionless groups, becomes:

10) $$\frac{d\Psi_D}{dx_D} = \frac{\pi}{4}$$

Notice that no specification of rate or pressure has been made. Normally, this expression is obtained by imposing the assumption of constant mass rate. However, it will be seen shortly that the only boundary requirement is stated above, that the derivative of the dimensionless potential (pressure) be constant at the sandface.

The LaPlace Transformation.

If the dimensionless pseudo-potential is piecewise regular and of exponential order (no shock waves and varies no faster than e^{ax}), the integration can be performed using the LaPlace Transformation (exactly analogous to an economics net present value calculation), which yields:

11) $$\frac{\partial^2 L\left[\Psi_D\right]}{\partial x_D^2} = s\,L\left[\Psi_D\right]$$

This ordinary differential equation integrates to give:

12) $$L\left[\Psi_D\right] = a\,e^{-x_D\sqrt{s}} + b\,e^{x_D\sqrt{s}}$$

The two boundary conditions are now to be imposed to evaluate the constants of integration. The general field condition requires that $\Psi_D \forall 0$ as $x_D \forall 0$ or t_D goes to infinity which requires that b = 0, in the previous equation, so that:

13) $$L\left[\Psi_D\left(t_D\right)\right] = a\,e^{-x_D\sqrt{s}}$$

The LaPlace Transformation of the sandface

14) $$\frac{\partial L\left[\Psi_D\right]}{\partial x_D} = -\frac{\pi}{4s}$$

The remaining constant of integration is evaluated by setting the transformed boundary condition at x_D = 0, equal to the derivative of the previous equation, so that:

15) $$-\frac{\pi}{4s} = -a\sqrt{s}\; e^{-x_D\sqrt{s}}$$

The solution in LaPlace Transformation space is then:

16) $$L[\Psi_D] = \frac{\pi}{4}\; s^{-3/2}\; e^{-x_D\sqrt{s}}$$

The Result.

The inverse transformation permits the evaluation of the dimensionless pseudo-potential as a function of dimensionless position. It has the form:

17) $$\Psi_D(t_D) = \frac{\pi}{4}\left[2\sqrt{\frac{t_D}{\pi}}\; e^{-\frac{x_D^2}{4t_D}} - x_D\, erfc\left(\frac{x_D}{2\sqrt{t_D}}\right)\right]$$

or at the sandface, where x_D = 0, so the result simplifies to:

18) $$\Psi_D(t_D) = \frac{\pi}{2}\sqrt{\frac{t_D}{\pi}}$$

By reintroducing the dimensionless groups and simplifying, the following results:

19) $$\frac{\Psi_i - \Psi_w(t)}{q_s(t)} = \frac{\rho_s}{\sqrt{\pi}\; kh}\sqrt{\frac{kt}{\Phi\mu\; c\, x_f^2}}$$

whose left-hand side has the form of the reciprocal of the productivity index, hence the name of the method.

TABLE 1
Comparison of Reservoir Parameters determined from RPI and Buildups on Example #1

Parameter	RPI Method	First Buildup	Second Buildup
Effective Permeability (mDs)	0.111	0.192	0.238
Fracture Length (ft.)	40	15	12
Initial Pressure (PSIA)	3532	3531	3359

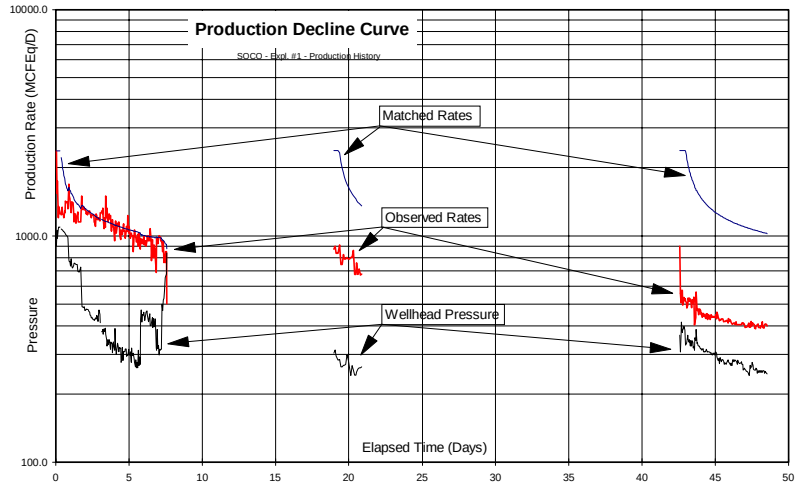

Fig. 1. Example #1 Observed and matched production and wellhead pressures

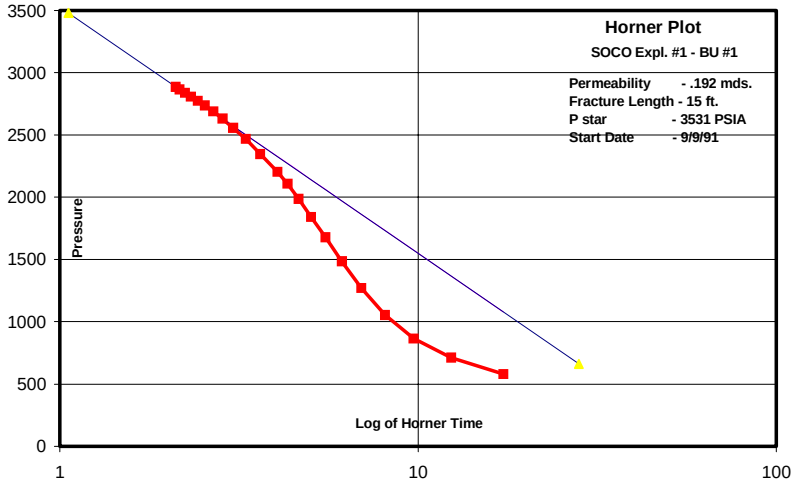

Fig. 2. Example #1 First Build-up Test

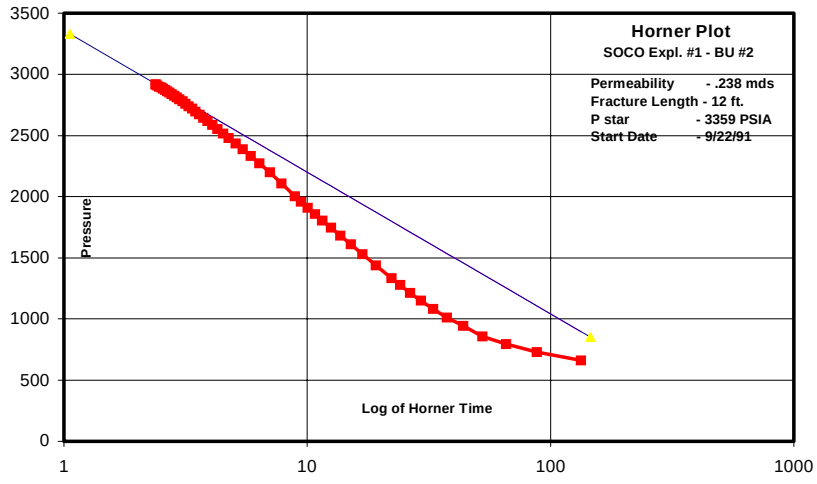

Fig. 3. Example #1 Second Build-up Test

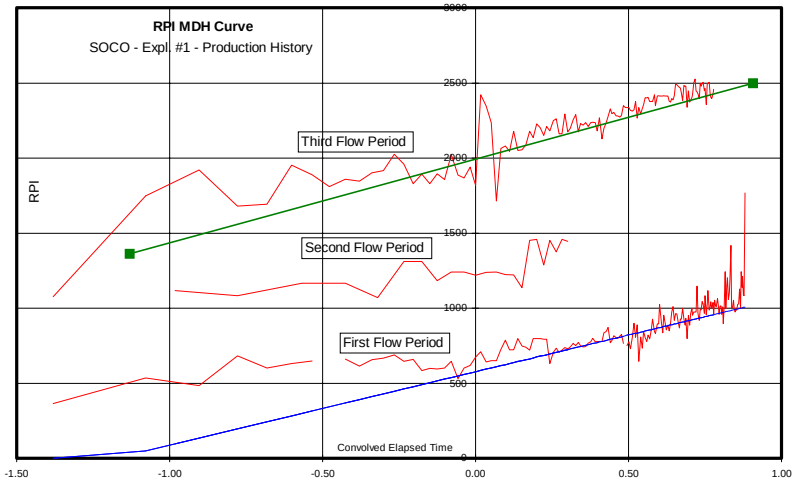

Fig. 4. Example #1 MDH Plot for RPI Analysis

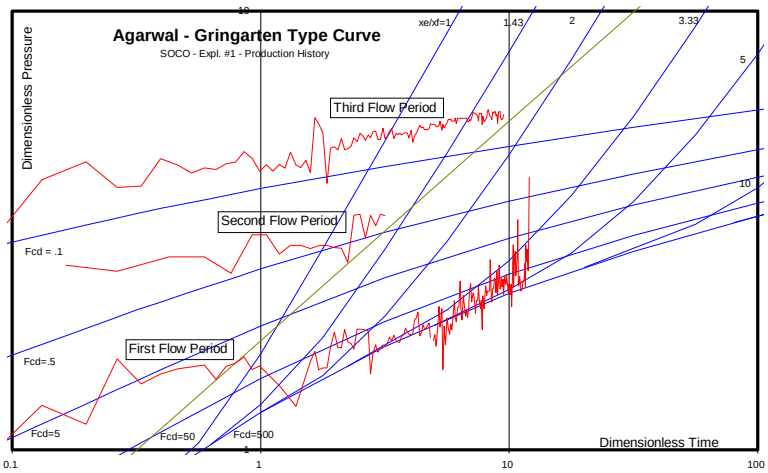

Fig. 5. Example #1 Agarwal-Gringarten Type Curve for RPI Analysis.

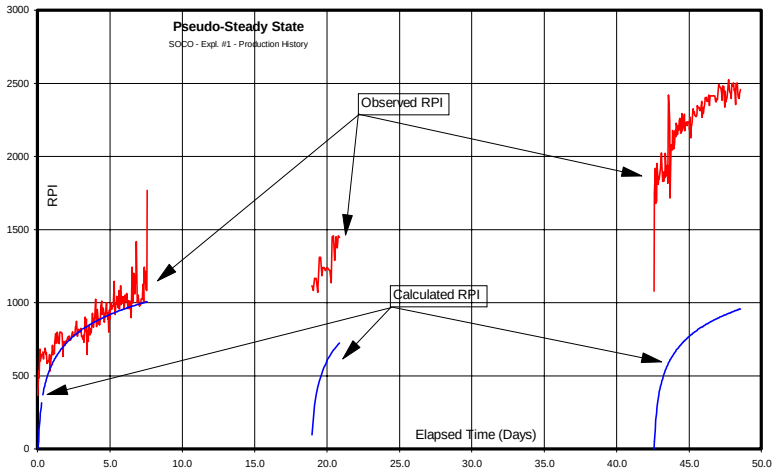

Fig. 6. Example #1 Cartesian pseudo-steady state plot.

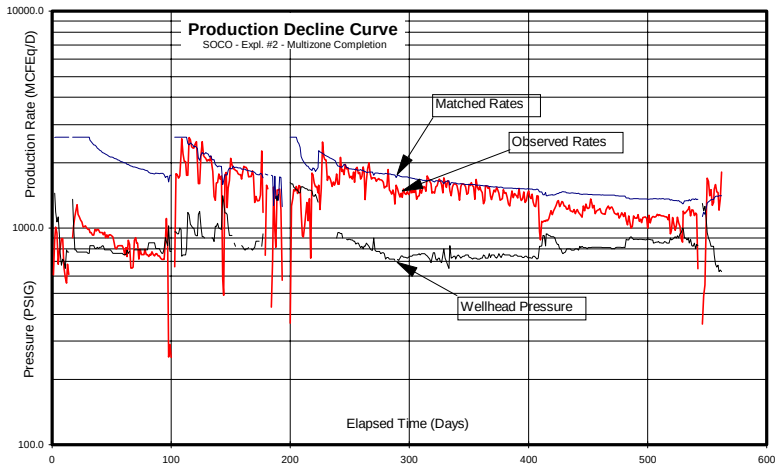

Fig. 7. Production and pressure history for multizone, multistage Example #2

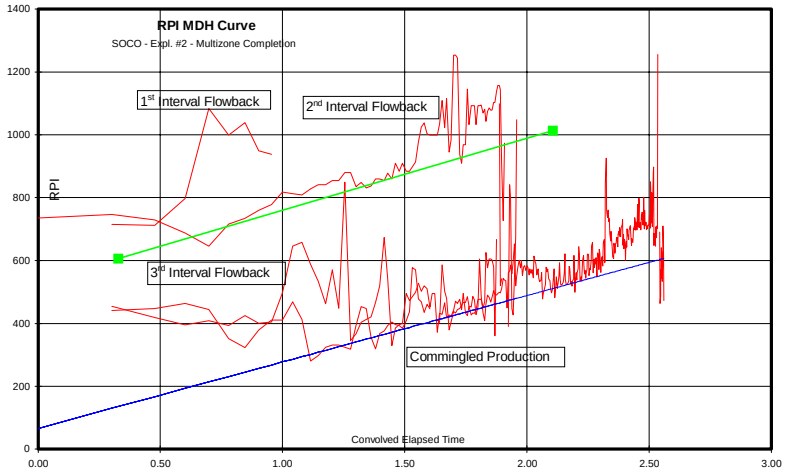

Fig. 8. MDH Plot for RPI of multizone, multistage Example #2

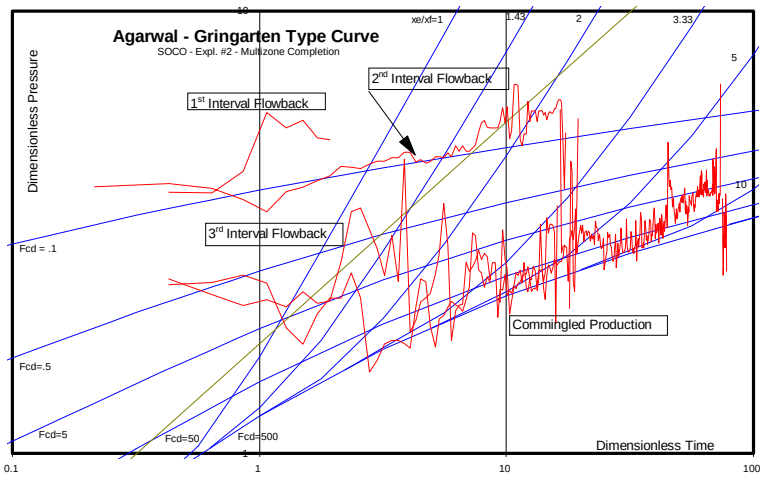

Fig. 9. Agarwal-Gringarten Plot for multizone, multistage Example #2.

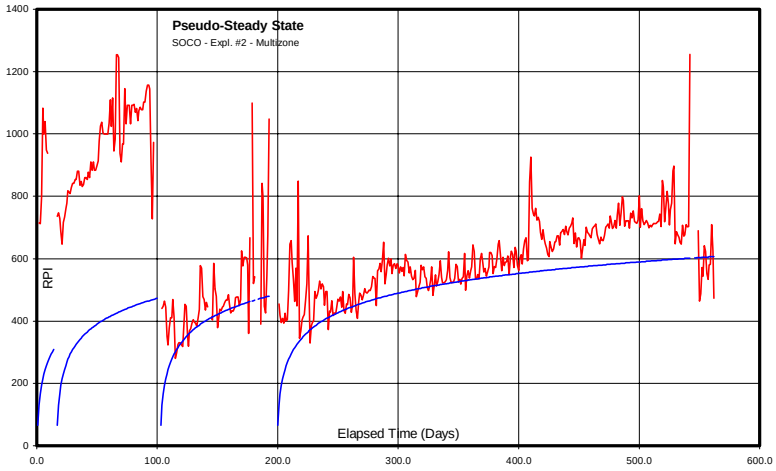

Fig. 10. Pseudo-steady state plot for multizone, multistage Example #2

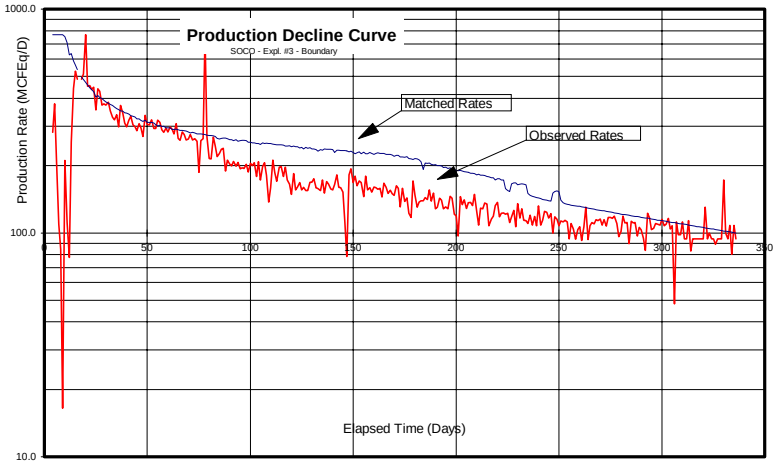

Fig. 11. Production history for Example #3.

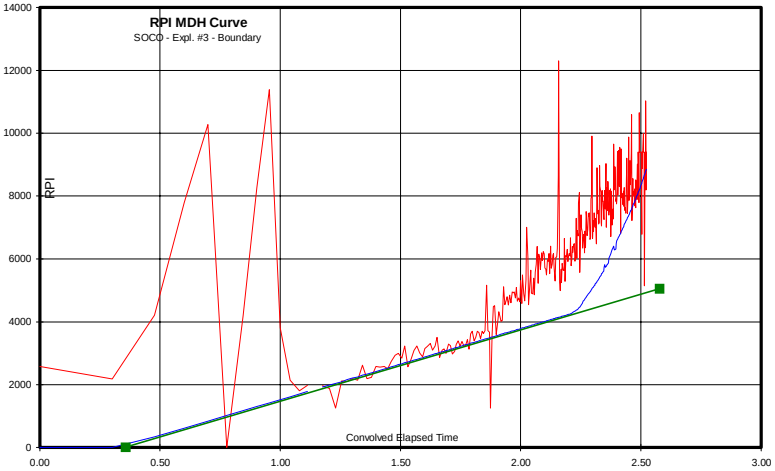

Fig. 12. The MDH Plot for Example #3.

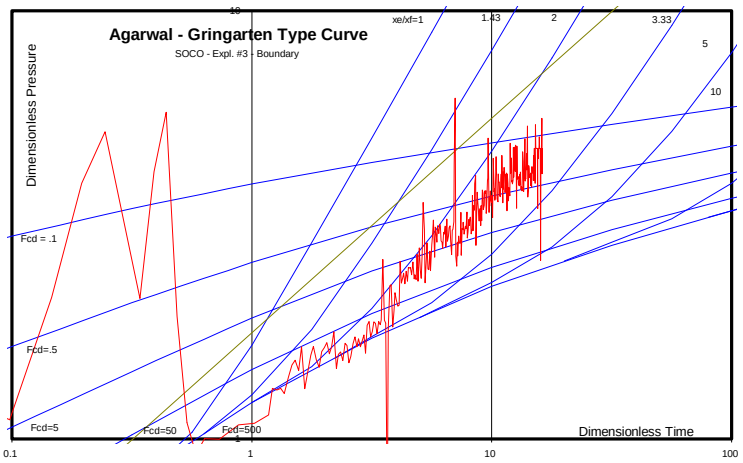

Fig. 13. The Agarwal-Gringarten Plot for Example #3.

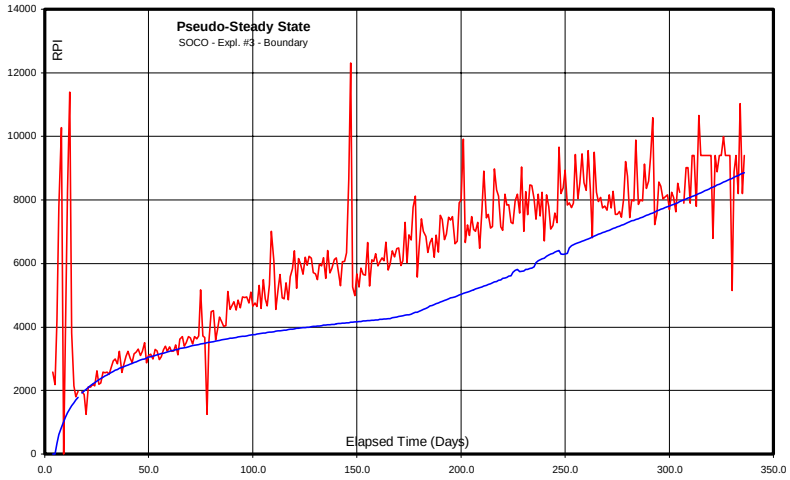

Fig. 14. The Pseudo-steady state plot for Example #3.

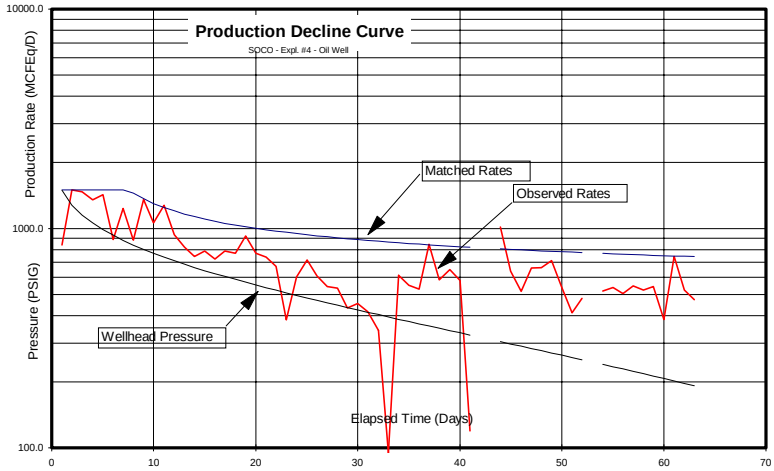

Fig. 15. Production and pressure history for the oil well in Example #4.

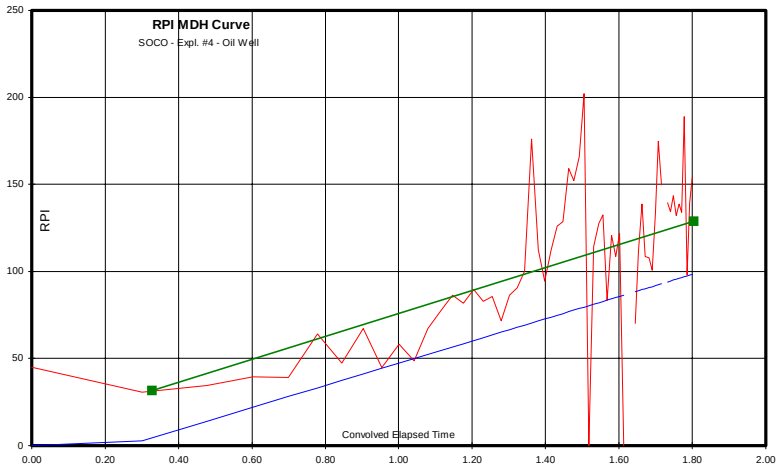

Fig. 16. The MDH Plot for Example #4.